

Internal-Gravity Waves Observed During the August 21, 2017 Total Solar Eclipse by National Eclipse Radiosonde Campaign

Katherine R. Stocker, * and Jennifer Fowler.¹
University of Montana, Missoula, Montana, 59801, United States.

Internal gravity waves are oscillations of a fluid parcel about an equilibrium level generated by a buoyancy force when the stability of the fluid medium is disrupted. Such a disturbance occurs from the obstruction of solar irradiance during a solar eclipse and may generate a gravity wave that can be detected using radiosondes. In this study, surface and upper air measurements made from a series of radiosondes launched throughout the duration of the August 21, 2017 total solar eclipse over the US as part of the National Eclipse Ballooning Project are examined for eclipse-induced gravity-wave activity. Preliminary results of radiosonde wind data collected throughout the eclipse from multiple sites within the path of totality in Wyoming reveal wave-like structures with intrinsic angular frequencies ranging $3.3 - 4.2 \times 10^{-2} \text{ s}^{-1}$ at altitudes within 18-20 km. The results of the wind data analysis presented here can be compared to results produced by wavelet analysis to either confirm or deny the generation of an eclipse-induced gravity-wave. Identifying the wave's structure would aid in wave prediction software to improve weather forecast models.

Nomenclature

u	=	Zonal wind ms^{-1} (<i>from west is negative, from east is positive</i>)
v	=	Meridional wind ms^{-1} (<i>from north is positive, from south is negative</i>)
w	=	Vertical ascent rate ms^{-1} (<i>increasing is positive, decreasing is negative</i>)
f	=	Coriolis frequency s^{-1}
N	=	Brunt-Väisälä frequency s^{-1}
ω	=	Intrinsic angular frequency $\times 10^{-2} \text{ s}^{-1}$
α	=	Propagation angle of wave radians

x' = Zonal wind perturbation m

* Post-baccalaureate, Physics & Astronomy Dept.

¹ MSGC Assistant Director, AASO Director, Physics & Astronomy Dept.

y' = Meridional wind perturbation m

z' = Vertical perturbation m

I. Introduction

A total solar eclipse occurs when the Moon passes between the Earth and the Sun and casts a shadow onto the surface of the Earth. The first total solar eclipse to span the United States from coast to coast in nearly 100 years occurred on August 21, 2017 and presented a path of totality from Oregon to South Carolina. A nationwide campaign was organized by the Montana Space Grant Consortium (MSGC) to capture live images of the eclipse from the edge of space using large high altitude balloons. Fifty-five student lead teams from across the US launched a common camera payload developed by the Montana State University (MSU) Balloon Outreach, Research, Exploration, and Landscape Imaging System (BOREALIS) team from multiple locations within the path of totality. “The National Eclipse Ballooning Project” included atmospheric measurements by radiosondes from more than 10 teams. The campaign aimed to monitor the planetary boundary layer and detect effects generated within the Troposphere and Stratosphere at different times throughout the eclipse. The University of Montana (UM) BOREALIS team structured high altitude radiosonde soundings to span the duration of the eclipse in an effort to detect a gravity wave within the atmosphere directly attributable to the cooling region of the moon’s shadow.

Chimonas theorized the generation of internal gravity waves about the shadow region of the eclipse from a distinct heating region 45 km into Earth’s continuously stratified atmosphere. The 3-dimensional perturbations are analogous to a ‘bow wave’ structured around the source [1]. During a total solar eclipse, gravity waves generated by the supersonic motion of the umbra through the atmosphere by analogy would propagate away from the shadow with largest perturbations centered around 45 km. The UM radiosonde team operated from three launch sites along the width of the path of totality near Fort Laramie, Wyoming with students from UM, MSU, and Miles City Community College (MCC). This study works to identify and analyze the gravity-wave structure in the upper air radiosonde observations collected from each of these three launch sites.

II. Methodology

The three UM radiosonde launch sites are designated as “North” edge (42.752 N, 104.456 W), “Central” (42.277 N, 104.454 W), and “South” edge (41.915 N, 104.382 W). The shadow of totality spanned approximately 110 km (70 miles), making the separation between neighboring sites no more than 55 km. A total of 19 radiosondes were launched over the course of 48 hours between the 3 launch sites. On the day of the eclipse, each site launched four radiosondes in conjunction with each other at the times listed in Table 1. A complete list of radiosonde flight information is displayed in Table 2. To avoid erroneous data transmission between multiple radiosondes aloft at one time, each radiosonde was assigned its own transmitting frequency during initialization, with a 200.0 kHz spacing between each.

Table 1 Launch times for site 1-3 on August 21, 2017

	<i>5 min Before 1st Contact</i>	<i>40 min Before Totality</i>	<i>5 min Before Totality</i>	<i>30 min After Totality</i>
South	S1_30 min	S1_20 min	S1_Burst	S1_Burst
North	S2_30 min	S2_20 min	S2_Burst	S2_Burst
Central	S3_30 min	S3_20 min	S3_Burst	S3_Burst

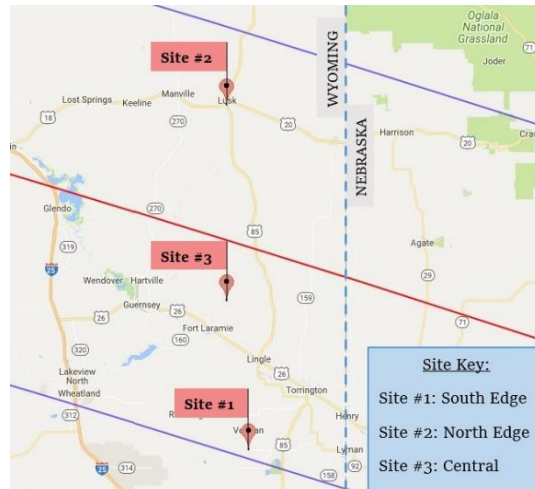


Fig. 1: Map of UM launch sites within the path of totality.

A. Surface Measurements

Conditions were measured at the surface of each radiosonde launch site. Center site near Fort Laramie recorded surface conditions using a Lufft WS502-UMB smart weather sensor and pyranometer beginning ~50 hours

prior to eclipse totality and ending approximately 24 hours after eclipse 4th contact. Figure 2 shows a 14 hour period of raw surface wind speed and temperature measurements compared to solar radiation between 06:00 and 20:00 MST on August 21, 2017. North and south edge sites in Lusk and near Veteran, respectively, recorded surface conditions using Kestrel 4500 and 5000 Pocket Weather Trackers. Error between Lufft and kestrel is small. Kestrels were calibrated and mounted on a tripod that allowed them to rotate freely with wind direction by attaching a wind vane to the mount. Kestrel data was continuously logged beginning ~ 3 hours prior to eclipse totality and ending ~ 2 hours after eclipse totality. Lufft and Kestrel measurements were used for surface values required by radiosonde software during initialization as well as to verify that a radiosonde's output was within desired specifications before each launch: $< \pm 5$ mb for pressure, $< \pm 2$ C for temperature, and $< \pm 10$ % for relative humidity.

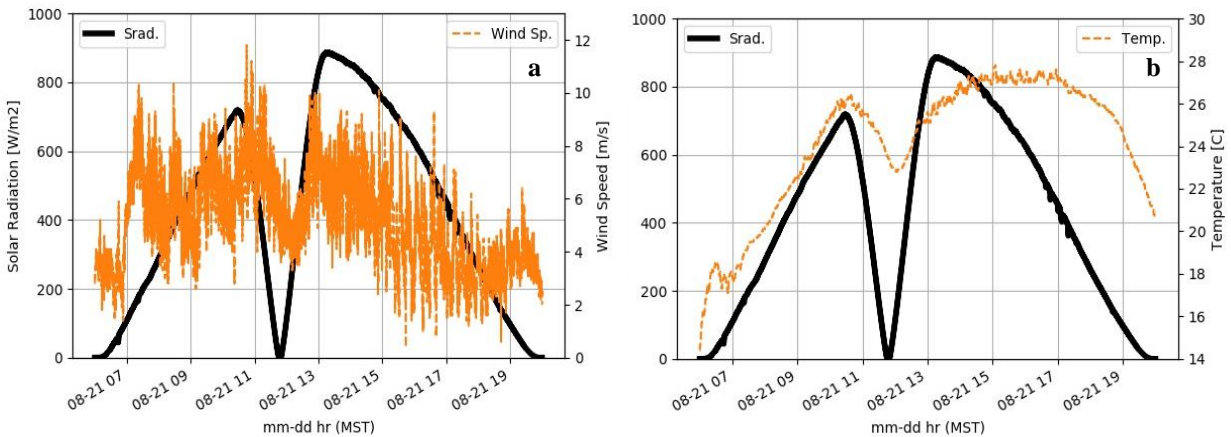


Fig. 2: Center site surface measurements of solar radiation vs a) wind speed and b) temperature.

B. Atmospheric Measurements

Upper air measurements were taken using GrawMet DFM -09 radiosondes suspended by 350 g or 1,000 g Kaymont latex high altitude weather balloons. The radiosonde is equipped with a temperature sensor designed to perform with resolution 0.1°C and accuracy of $\pm < 0.2^{\circ}\text{C}$ up to 40 km, a humidity sensor and code-correlated global positioning system (GPS) receiver. The GrawMet software uses the corresponding temperature and GPS readings to calculate pressure, wind speed, wind direction, altitude, and vertical rise rate. Each sounding gives high temporal resolution ($\delta t = 2$ second) vertical profiles of the parameters listed above. The balloons were filled with helium to achieve an average rise rate of 5 m/s for adequate air flow over the sensors. The fill value was dependent on balloon mass, payload mass, surface temperature, and surface pressure. After initialization, a radiosonde was allowed to hang approximately 3 feet off the ground and within 5 feet of the Kestrel or Lufft surface weather station at least 15 minutes to fully acclimate

to the surrounding conditions. The radiosonde is then attached to the weather balloon using 50 lb test string along with a parachute and a de-reeler containing ~29 meters of additional string. The top of the parachute is attached to the neck of the balloon with ~0.75 m of string. The de-reeler is attached to the bottom of the parachute with ~ 0.16 m of string and, lastly, the radiosonde is secured to the end of the string within the de-reeler. When the balloon is released and ascends into the atmosphere, the de-reeler slowly unwinds to create more than 30 meters of space between balloon and radiosonde to avoid wake affects from the balloon. GrawMet software corrects for pendulum effects experienced by the radiosonde shortly after release.

Table 2 Flight information from all radiosondes launched by UM.

Aug. 20, 2017					
	<u>Launch time w.r.t eclipse</u>	<u>ID</u>	<u>Launch</u>	<u>Terminate</u>	<u>Max Altitude ASL, m</u>
350 g	T/C2	N1	11:47 am	Burst	24,166
		S1	11:45:51 am		24,755
		C1	11:45:08 am		26,681
	18 hours before T	C2	05:49:08 pm		26,181
	12 hours before T	C3	11:46:04 pm		27,560
Aug. 21, 2017					
350 g	6 hours before T	C4	05:46:04 am	Burst	25,106
	5 min before C1	N2	10:18:57 am	~ 30 min	11,395
		S2	10:18:12 am		9,684
		C5	10:19:04 am		9,111
	40 min before T/C2	N3	11:06:01 am	~ 20 min	7,561
		S3	11:05:44 am	~ 50 min	16,570
		C6	11:06:05 am	~ 20 min	7,083
1000 g	5 min before T/C2	N4	11:40:56 am	Burst	31,682
		S4	11:40:56 am		32,435
		C7	11:41:08 am	~ 25 min	9,490
	30 min after T/C2	N5	12:16:55 pm	Burst	34,528
		S5	12:18:28 pm		32,241
		C8	12:16:04 pm		32,378
Aug. 22, 2017					
350 g	T/C2	C9	11:47:30 am	Burst	26,616

Radiosonde profiles N2, N3, S2, C5, and C6 were terminated before totality and before reaching the stratosphere. For these reasons, analysis of these profiles will be left for planetary boundary layer studies and will not be presented here.

C. Analysis

Analysis of each radiosonde sounding was applied in two steps. To first extract wave signal from the soundings, a filtering method presented by Scavuzzo [3] is applied to the horizontal and vertical raw wind profiles to isolate waves with intrinsic frequencies between the Coriolis frequency f and the Brunt-Väisälä frequency N . The moving parcel method described by Marlton [2] is then applied to the filtered data to quantify wave frequency, amplitude and wavelength of the dominant wave signal. The angle of the winds with altitude are examined to reveal energy dissipation and propagation direction. To begin the analysis, a linear spline is applied to transform the irregularly spaced vertical profiles of temperature, pressure and wind into regular ones with resolution $\delta z \cong 10$ m. The filtering process works by first applying a low-pass filter that suppresses frequencies smaller than f . A second low pass filter that suppresses frequencies smaller than the approximate upper bound of N is applied to the resulting signal from the first filter. The complete filtered wave signal is obtained as the difference between the two filtered signals. Typical values of N below 50 km are on the order of 10^{-2} s^{-1} . N was calculated for each sounding from the thermodynamic variables measured by the radiosonde over a 250 m height window, Marlton [2]. The value of f varies slightly between each launch site due to their different latitudes. Due to drift experienced by the radiosonde during flight, the value of f experienced at the north edge site, south edge site, and center is averaged to be $9.87 \times 10^{-5} \text{ s}^{-1}$, $9.74 \times 10^{-5} \text{ s}^{-1}$ and $9.81 \times 10^{-5} \text{ s}^{-1}$, respectively.

In a stably stratified fluid, the restoring buoyancy force for fluid parcel oscillation is always transverse to the propagation of the wave. The phase of the wave is a function of height, and the exact intrinsic angular frequency ω of the gravity wave can be calculated using:

$$\omega^2 = f^2(\sin \alpha)^2 + N^2 (\cos \alpha)^2 \quad (1)$$

where α is the propagation angle of the wave, also known as the angle that the wave number vector makes with the horizontal plane. This equation is commonly referred to as the wave dispersion relation. In terms of the three-dimensional displacements of an air parcel, α is defined as:

$$\alpha = \tan^{-1}\left(\frac{\sqrt{x'^2 + y'^2}}{|z'|}\right). \quad (2)$$

To calculate the displacements, a second-order polynomial was fitted to the filtered u , v , and w wind components from each profile to calculate background velocities. The background and filtered velocities are then integrated to generate mean and filtered displacements. The mean displacements are then subtracted from the filtered displacements to calculate the perturbations x' , y' , and z' . These displacements yield frequency and wavelength of the wave signal.

III. Observations

Maximum eclipse at occurred at 11:46:18 MST at center site with only seconds difference between maximum eclipse experienced at north and south edge sites. The first set of radiosondes were launched 24 hours prior to totality at each site and allowed to enter the stratosphere. Figure 3 displays unfiltered u , v and temperature within the troposphere from these soundings. A shift in wind direction seen at roughly 2 km at each site corresponds to a temperature inversion at this altitude, marking a PBL. A predominantly south-westerly wind is present in each sounding with peak amplitude centered around 14 km. Its magnitude is nearly 10 m/s greater than the wind speeds recorded 4 km above and below and nearly 20 m/s greater than wind speeds recorded near the surface and above 18 km. These observations are common for mid-latitude soundings due to the presence of the ferrel westerly cell. The vertical profiles collected every 6 hours from the center site also display these characteristics. Above 18 km, the oscillations observed in u and v reveal 180° counter-clockwise wind rotation occurring over a vertical distance of 6 km in the daytime while rotations diminish to less than 45° counter-clockwise at night.

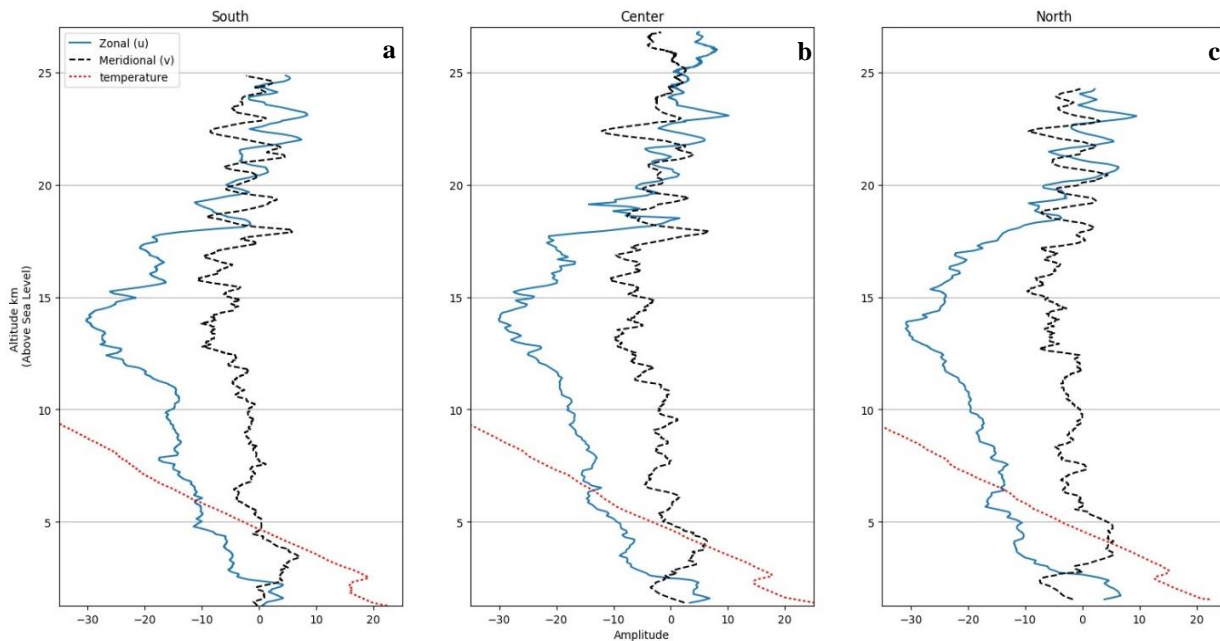


Fig. 3: Unfiltered u (solid), v (dashed), and temperature [C] (dotted) data from a) S1, b) C1, and c) N1

Each profile of horizontal wind and vertical ascent speed collected within 24 hours of eclipse totality were filtered to isolate a pre-eclipse wave signal. Figure 4 displays the filtered wind profiles of u and v from each site 24 hours

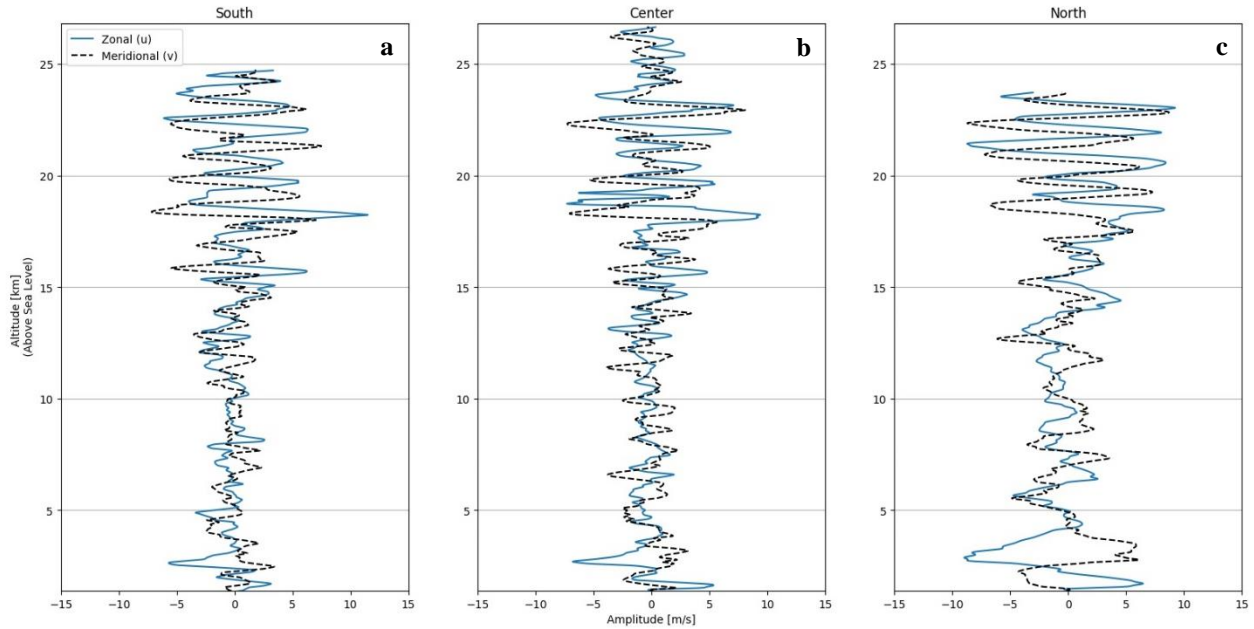


Fig. 4: Filtered u (solid) and v (dashed) from a) S1, b) C1 and c) N1.

prior to eclipse totality. A spike in winds from the west with phase opposition between the wind components u and v around 2 km provides a qualitative indication of high intrinsic frequency. Consistent phase opposition between u and v is found every 6 hours in the filtered center wind profiles C1– C4 within 5 to 7 km. Above the ferrel westerly cell and into the stratosphere, larger amplitude peaks of u and v are seen to be roughly half cycle out of phase at 18 km, shifting to one quarter out of phase with increasing altitude and eventually in phase around 20 km. These signatures correspond to the peaks seen in the raw profiles and indicate decreasing intrinsic frequency with altitude.

The frequency of the wave signal from the filtered profiles 24 hours prior to eclipse totality are shown in figure 5. The lowest intrinsic angular frequencies are centered on altitudes of 2, 6, and 17 km. The higher frequencies concentrated around 10 km arise from the large perturbations calculated within the ferrel cell. Between 18 and 25 km, the intrinsic angular frequency approximately averages to $1 \times 10^{-2} \text{ s}^{-1}$. Filtered profiles C2, C3, and C4 leading up to the eclipse display similar frequency patterns with additional local minimums in frequency centered around 19 and 21 km appearing at night. The profiles of radiosondes from the north and south edge sites that were allowed to ascend

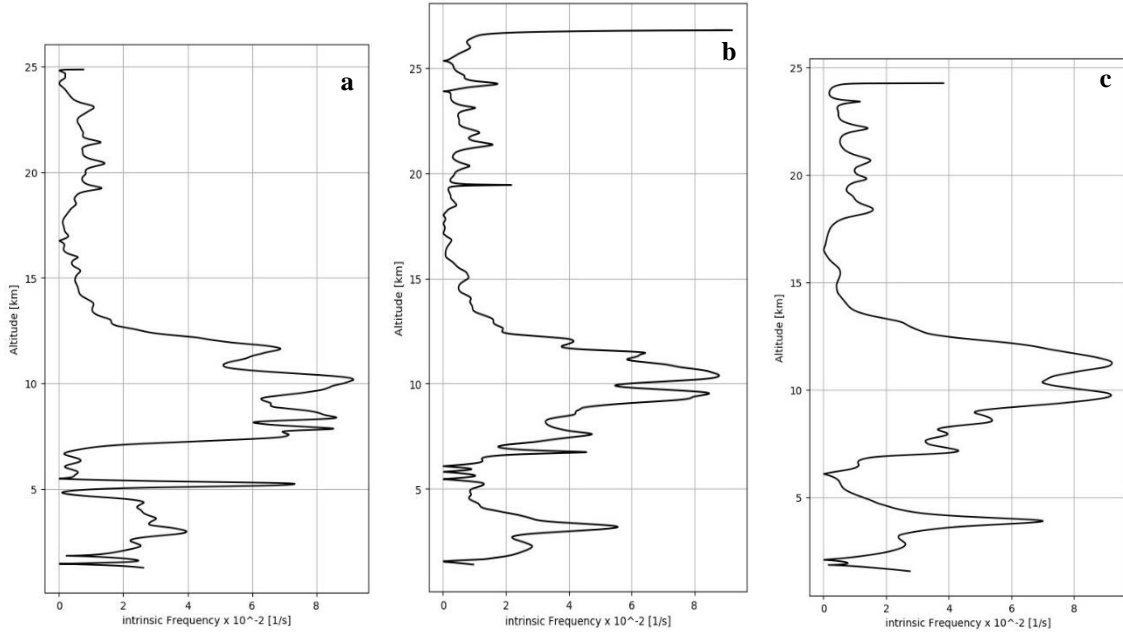


Fig. 5: Intrinsic angular frequency from a) S1, b) C1, and c) N1.

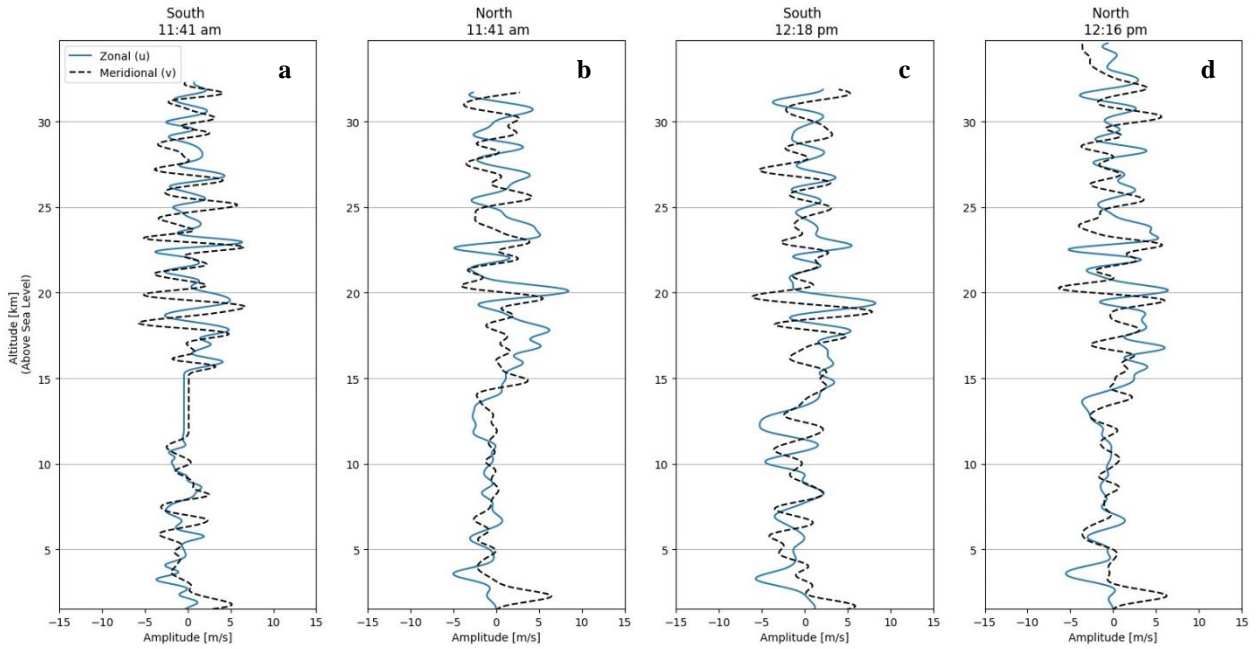


Fig. 6: Filtered u (solid) and v (dashed) from a) S4, b) N4 and c) S5, d) N5.

into the stratosphere post-totality (N4, N5, S4 and S5) are presented in figure 6. These radiosondes were launched with a 1,000 g latex balloon and reached heights not spanned prior to the eclipse. Therefore, comparisons for eclipse-generated wave-structures at altitudes greater than 27 km cannot be made.

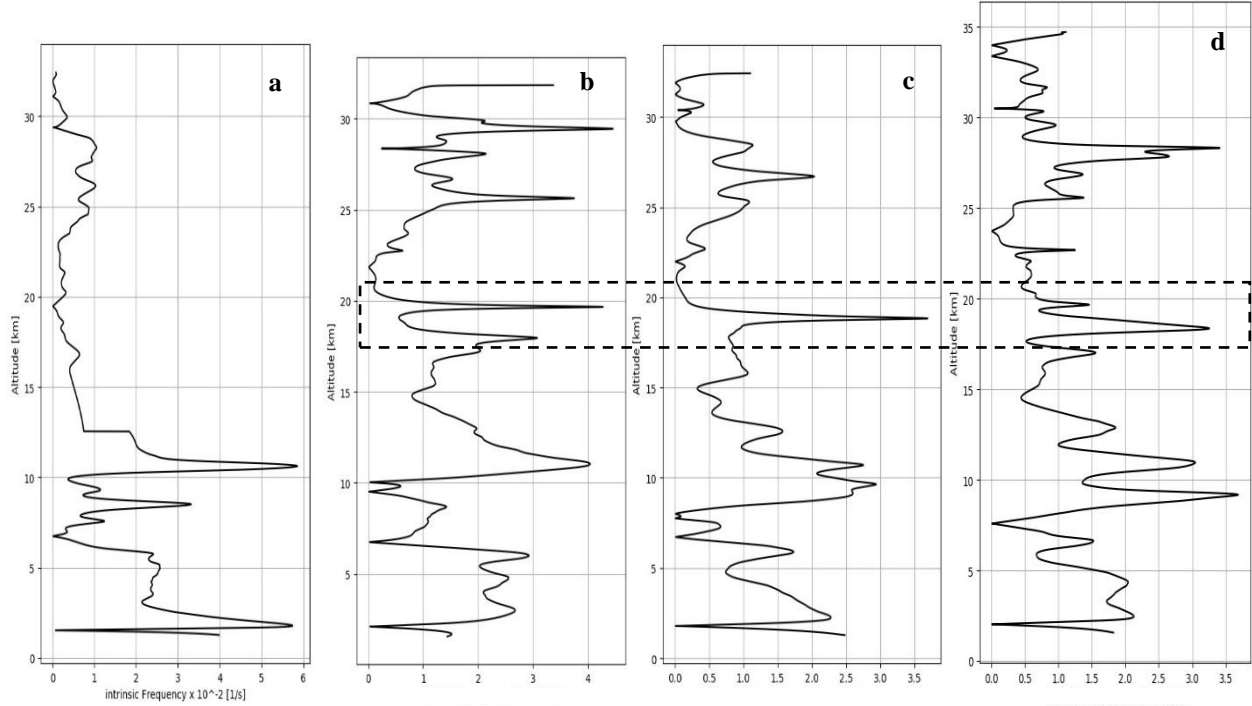


Fig. 7: Filtered intrinsic angular frequency $\times 10^{-2} \text{ s}^{-1}$ from a) S4, b) N4, c) S5, and d) N5.

Figures 6 and 7 display post-totally results of horizontal wind components and intrinsic angular frequency. The amplitudes of the oscillations in u and v above 18 km have diminished by half. The large frequencies centered around 10 km 24 hours prior have reduced by nearly 60%. A wave signal is first detected at 19.5 km approximately 50 minutes after totality in N5. The large frequency spike indicates a dominant intrinsic angular frequency of $\sim 4.2 \times 10^{-2} \text{ s}^{-1}$. Due to erroneous data transmission that occurred while S5 was spanning this altitude, a similar spike was not detected in this sounding. However, a similar signal is detected again 30 minutes later at both edge sites at altitude ~ 19 km with slightly lower frequency $\sim 3.6 \times 10^{-2} \text{ s}^{-1}$ in S5 and $\sim 3.3 \times 10^{-2} \text{ s}^{-1}$ in N5. These frequencies correspond to vertical wavelengths of ~ 20 m. Twenty-four hours following totality in C9, a frequency spike with comparable amplitude is absent at this altitude. Wind direction measurements reveal clockwise rotation below 19 km and anticlockwise above, indicating upward and downward wave energy propagation.

Analysis of UM's sequential radiosonde profiles during the August 21, 2017 total solar eclipse reveal a dominant gravity-wave structure located around 19 km with initial intrinsic angular frequency approximately $4.2 \times 10^{-2} \text{ s}^{-1}$ and vertical wavelength ~ 20 m. Wind rotation above and below indicate energy propagation centered from this altitude. The number of frequencies excited post totality suggest complex interaction and possible superposition between gravity waves. The absence of such a significant wave structure in the soundings leading up to totality and

the sounding taken 24 hours after suggest that the wave structure is likely eclipse-induced with finite period. The results of the wind data analysis presented here can be compared to results produced by wavelet analysis to further investigate these preliminary findings.

References

- [1] Chimonas G, "Internal-Gravity Wave Motions Induced in the Earth's Atmosphere by a Solar Eclipse." *J. Geophys. Res.* 75. 1970.
- [2] Marlton GJ, Williams PD, Nicoll KA. "On the detection and attribution of gravity waves generated by the 20 March 2015 solar eclipse." *Phil. Trans. R. Soc. A* **374**: 20150222. 2016
- [3] Scavuzzo, C. M., M. A. Lamfri, H. Teitelbaum, and F. Lott. "A study of the low-frequency inertio-gravity waves observed during the Pyrénées Experiment." *J. Geophys. Res.*, 103(D2), 1747–1758, doi:10.1029/97JD02308. 1998.